



# Lithium-ion (de)intercalation mechanism in core-shell layered Li(Ni,Co, Mn)O<sub>2</sub> cathode materials

Weibo Hua<sup>a,b,\*</sup>, Björn Schwarz<sup>b,\*\*</sup>, Raheleh Azmi<sup>b</sup>, Marcus Müller<sup>b</sup>,  
 Mariyam Susana Dewi Darma<sup>b</sup>, Michael Knapp<sup>b</sup>, Anatoliy Senyshyn<sup>c</sup>, Michael Heere<sup>b,c</sup>,  
 Alkesandr Missyul<sup>d</sup>, Laura Simonelli<sup>d</sup>, Joachim R. Binder<sup>b</sup>, Sylvio Indris<sup>b,\*\*\*</sup>,  
 Helmut Ehrenberg<sup>b</sup>

<sup>a</sup> State Key Laboratory of Electronic Thin Films and Integrated Devices, University of Electronic Science and Technology of China, Chengdu, 610054, China

<sup>b</sup> Institute for Applied Materials (IAM), Karlsruhe Institute of Technology (KIT), Hermann-von-Helmholtz-Platz 1, 76344, Eggenstein-Leopoldshafen, Germany

<sup>c</sup> Heinz Maier-Leibnitz Zentrum, Technische Universität München, Lichtenbergstrasse 1, D-85747, Garching, Germany

<sup>d</sup> CELLS-ALBA Synchrotron, Cerdanyola del Valles, E-08290, Barcelona, Spain

## ARTICLE INFO

### Keywords:

Core-shell architecture  
 Coexisting layered phases  
 Chemical composition  
 (de)Lithiation mechanism

## ABSTRACT

LiNi<sub>x</sub>Co<sub>y</sub>Mn<sub>1-x-y</sub>O<sub>2</sub> (NCM) intercalation compounds with core-shell architecture have been found to be promising cathode candidates for next-generation lithium-ion battery applications. The NCM cathodes' functional properties are dependent on the transition metal relative ratios, making it a challenge to control the real structure of core-shell NCM cathode materials and to understand the synergistic effect of core and shell during the electrochemical cycling. Herein, a universal and facile synthetic strategy is developed to synthesize the NCM material composed of an inner Ni-rich core and a Mn-rich shell on a secondary particle level. Both the Ni-rich particle core and the Mn-rich outer surface possess a layered  $\alpha$ -NaFeO<sub>2</sub>-type structure with the same space group ( $R\bar{3}m$ ). The *in situ* synchrotron-based X-ray diffraction and absorption spectroscopy results demonstrate that the two layered phases do not participate in the electrochemical reaction simultaneously during the first cycle between 2.7 and 4.3 V, while they exhibit a similar reversible (de)lithiation mechanism in the following cycles. These findings provide a new perspective for rational design of layered Ni-based cathode materials with high energy and long cycling life with particular two phase electrochemical characteristics.

## 1. Introduction

Achieving green energy technology application in energy storage systems (ESS) [1–3] and electric vehicles (EVs) is imperative to develop the next-generation cathode materials in lithium ion batteries (LIBs) [4–8]. To reach such goals, present research mainly focuses on the development of metal-O<sub>2</sub>/CO<sub>2</sub> batteries [9,10], the preparation of new iron-based poly-anionic compounds [11,12], and the improvement of existing layered lithium-containing transition-metal oxides (LiNi<sub>x</sub>Co<sub>y</sub>Mn<sub>1-x-y</sub>O<sub>2</sub>, abbreviated as NCM) [13–15]. The metal-O<sub>2</sub>/CO<sub>2</sub>

cathodes have a substantially high theoretical capacity but these materials are still far from being considered for practical applications because of their low working voltage. The poly-anionic compounds, e.g., the intensively investigated LiFePO<sub>4</sub>, show a good cycling stability due to the stabilization of oxygen anions via strong covalent bonds of poly-anions in the crystal structure [16,17]. The intrinsically poor bulk electronic and ionic conductivities of these compounds result in an inferior rate capability [18,41]. Currently, modified layered NCM cathodes could deliver the highest capacity (>200 mA h g<sup>-1</sup>) of cathode materials utilized up-to-date, which would make them interesting

\* Corresponding author. State Key Laboratory of Electronic Thin Films and Integrated Devices, University of Electronic Science and Technology of China (UESTC), Chengdu, 610054, China.

\*\* Corresponding author. Institute for Applied Materials (IAM), Karlsruhe Institute of Technology (KIT), Hermann-von-Helmholtz-Platz 1, 76344 Eggenstein-Leopoldshafen, Germany.

\*\*\* Corresponding author. Institute for Applied Materials (IAM), Karlsruhe Institute of Technology (KIT), Hermann-von-Helmholtz-Platz 1, 76344 Eggenstein-Leopoldshafen, Germany.

E-mail addresses: [weibo.hua@uestc.edu.cn](mailto:weibo.hua@uestc.edu.cn), [weibo.hua@kit.edu](mailto:weibo.hua@kit.edu) (W. Hua), [bjoern.schwarz@kit.edu](mailto:bjoern.schwarz@kit.edu) (B. Schwarz), [sylvio.indris@kit.edu](mailto:sylvio.indris@kit.edu) (S. Indris).

<https://doi.org/10.1016/j.nanoen.2020.105231>

Received 9 April 2020; Received in revised form 29 June 2020; Accepted 25 July 2020

Available online 12 August 2020

2211-2855/© 2020 The Authors.

Published by Elsevier Ltd.

This is an open access article under the CC BY-NC-ND license

(<http://creativecommons.org/licenses/by-nc-nd/4.0/>).

candidates for next-generation LIBs [19–22].

Layered NCM oxides possess a trigonal  $\alpha$ -NaFeO<sub>2</sub>-type structure with space-group symmetry of  $R\bar{3}m$ . These can be considered as an ordered rock-salt ( $Fm\bar{3}m$ ) derivative, where the lithium ions and transition-metal (TM) cations are located on octahedral sites of alternating layers forming LiO<sub>6</sub> and TMO<sub>6</sub> octahedra, respectively, see Fig. S1 in the electronic supplementary information (ESI). Among the series of NCM compounds, a high nickel concentration is beneficial for the enhancement of specific capacity, high cobalt content is favourable for improving the rate performance and high manganese content could conduce to enhance the structural stability [23–25]. Recently, Sun et al. [26,27] have suggested that the controlled preparation of a Mn-rich shell surrounding a Ni-rich core is an efficacious approach to improve the cycling stability of NCM cathodes during electrochemical testing. However, the intercalation/de-intercalation mechanism of lithium ions into/from core-shell-architected NCM cathode materials is not very clear. One open question is whether both phases are intercalated/deintercalated subsequently or simultaneously.

In this work, a core-shell NCM material was successfully synthesized by using a facile and scalable hydroxide co-precipitation method. The prepared NCM material possesses a layered Ni-rich core and a layered Mn-rich shell on a secondary particle level. Both these layered compounds have a rhombohedral crystal structure, space group ( $R\bar{3}m$ ), but subtle difference in the lattice parameters. Moreover, we focus on how non-equilibrium (de)lithiation reactions proceed in the core-shell-architected NCM cathode. The variation of the lattice parameters of two phases is not simultaneously during the first cycle, such discrepancy become negligible in subsequent cycles. This study provides new insights into the synergistic effect of the peculiar core-shell architecture in positive NCM electrodes.

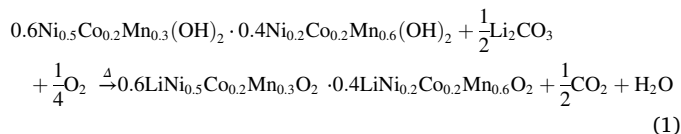
## 2. Results and discussion

On the basis of our previous work [28–30], a co-precipitation method was employed to obtain core-shell structured NCM cathode materials, as shown in Fig. S2. A Ni-rich aqueous solution made of NiSO<sub>4</sub>·6H<sub>2</sub>O, CoSO<sub>4</sub>·7H<sub>2</sub>O and MnSO<sub>4</sub>·H<sub>2</sub>O at a molar ratio of 5:2:3 was fed into a reactor Nr.1. Simultaneously, a sodium hydroxide solution (aq.) and a desired amount of NH<sub>4</sub>OH solution (aq.) were successively added into the reactor Nr.1. After the nucleation/crystallization process, the precipitates formed in reactor Nr.1 were slowly pumped into a reactor Nr.2 as crystal nuclei. Subsequently, a Mn-rich solution composed of NiSO<sub>4</sub>·6H<sub>2</sub>O, CoSO<sub>4</sub>·7H<sub>2</sub>O and MnSO<sub>4</sub>·H<sub>2</sub>O (cationic molar ratio of 2:2:6), a NaOH solution and an ammine solution were added into the reactor Nr.2. The pH value (11.3 ± 0.2), reaction temperature (52 ± 2 °C) and stirring speed (700 rpm) were carefully controlled during the reaction process, see electronic supplementary information (ESI) for more details. The molar ratio of the Ni-rich solution and Mn-rich solution is 3:2. The precipitated precursor was filtered, washed and dried to remove impurity ions and adsorbed water. The precursor obtained from reactor Nr.1 and reactor Nr.2 are marked as precursor-1 and precursor-2, respectively.

Both precursor-1 and precursor-2 particles are spherical agglomerates composed of thin nanoplates, see Fig. S3. A core-shell structured precursor-2 including a Mn-rich shell and a Ni-rich core was directly observed by cross-sectional scanning electron microscopy (SEM) image and by energy-dispersive X-ray spectroscopy (EDX) line-scan data, as shown in Fig. S4. That is, manganese is mainly distributed in the outer surface area whereas nickel is localized prominently in the interior region of a secondary particle. Cobalt is distributed homogeneously in both inner and outer part of the particle as the same concentration of cobalt is present in both reactors. Fig. S5 displays a particle size distribution of both precursors. The cumulative profile and corresponding histogram curve of precursor-2 shift to a larger particle size when compared with those of precursor-1, indicating that precipitated crystals

continue to grow or accumulate on the surface of precursor-1 in reactor Nr.2.

A core-shell NCM cathode material was synthesized via a high temperature lithiation reaction (1) ( $\Delta$  indicates heating):



For comparison, the components LiNi<sub>0.5</sub>Co<sub>0.2</sub>Mn<sub>0.3</sub>O<sub>2</sub> (NCM523) and LiNi<sub>0.2</sub>Co<sub>0.2</sub>Mn<sub>0.6</sub>O<sub>2</sub> (NCM226) were also prepared from the hydroxide precursor and lithium carbonate by using the same heating procedure. The microstructure and elemental distribution of the core-shell precursor could be preserved after the calcination process. The Ni-rich particle core and Mn-rich outer surface (of about 1 μm of thickness) are clearly seen from the SEM-EDX mapping images (Fig. 1(a–e) and Fig. S7). In particular, the Co content remains almost constant, the Ni concentration increases gradually from the particle surface to the particle center whereas the Mn concentration decreases concurrently (Fig. 1(f)). The elemental composition of Ni:Co:Mn in the surface and inner part of the core-shell precursor is roughly 0.23(5):0.25(5):0.52(5) and 0.55(5):0.23(5):0.22(5), see Fig. S4. After high-temperature lithiation reaction, these values become approximately 0.34(5):0.17(5):0.49(5) (shell) and 0.44(5):0.19(5):0.37(5) (core), respectively, suggesting an inter-diffusion of Ni and Mn during calcination driven by concentration gradient [31].

Surface chemical compositions and oxidation state of the core-shell NCM, NCM523 and NCM226 particles separately were investigated by X-ray Photoelectron Spectroscopy (XPS). The 2p spectra of Ni, Co, and Mn are shown in Fig. 2. The Ni 2p spectra consist of weak Mn LMM Auger, Ni2p satellites, and multiplets. According to the approach of Azmi et al. [32] the Ni ions in all three samples attributed to the Ni<sup>2+</sup> state whereas the NCM532 particles contain also a minor contribution of Ni<sup>3+</sup> ions, the spectra overlay of these 3 samples in Fig. S8 also shows a slightly broader FWHM for NCM532 in further confirmation of oxidation state assignment. The spectra of Co ions are all similar and show a characteristic structure of Co<sup>3+</sup> ions, normally found in LiCoO<sub>2</sub> compounds, with a main peak at 780.3 eV and a weak satellite peak at around 9 eV higher than the main peak (at 789.8 eV) [32,33]. Therefore, the Co ions in NCM523, NCM226, and core-shell NCM samples are attributed to the Co<sup>3+</sup> ions. The Mn 2p spectra in NCM226 and core-shell samples, in agreement with the splitting energy of 4.5 eV for Mn 3s spectra (see Fig. S8), could be successfully deconvoluted by using Mn<sup>4+</sup> set of multiplets and considering the overlapping Ni LMM Auger peaks [32,33]. However, the weak Mn 3s spectra (see Fig. S8) of NCM532 shows a splitting energy of around 5 eV which is mainly attributed to a mixed oxidation state [15,32,33] of Mn<sup>3+</sup> and Mn<sup>4+</sup> that could properly deconvolute the Mn 2p spectra of NCM532. The summary of oxidation states of transition metals and their surface elemental compositions quantified by XPS and normalized to Co being 0.2 is shown in Table 1. The normalized atomic percentages show that for a constant amount of Co, the core-shell secondary particles show Mn values near to the amount found for NCM226 particles whereas the Ni content is higher than NCM226 and lower than NCM523 particles so that Mn is enriched on the surface. Finally the overall chemical composition of the prepared core-shell material measured by inductively coupled plasma optical emission spectrometry (ICP-OES) demonstrates that its atomic ratios of Li:Ni:Co:Mn is around 1.00(2):0.37(2):0.19(2):0.43(2), which agrees well with the nominal value (1.00:0.38:0.20:0.42).

High-resolution synchrotron radiation powder diffraction (SRD) was used to investigate the crystallographic structure of NCM523 and NCM226. All the reflections in SRD pattern of NCM523 can be indexed according to a rhombohedral layered phase ( $R\bar{3}m$ ), see Fig. 3(a–b). In comparison to NCM523, several weak reflections over a 2θ range of 5.3–7.7° belonging to a honeycomb superstructure of a monoclinic

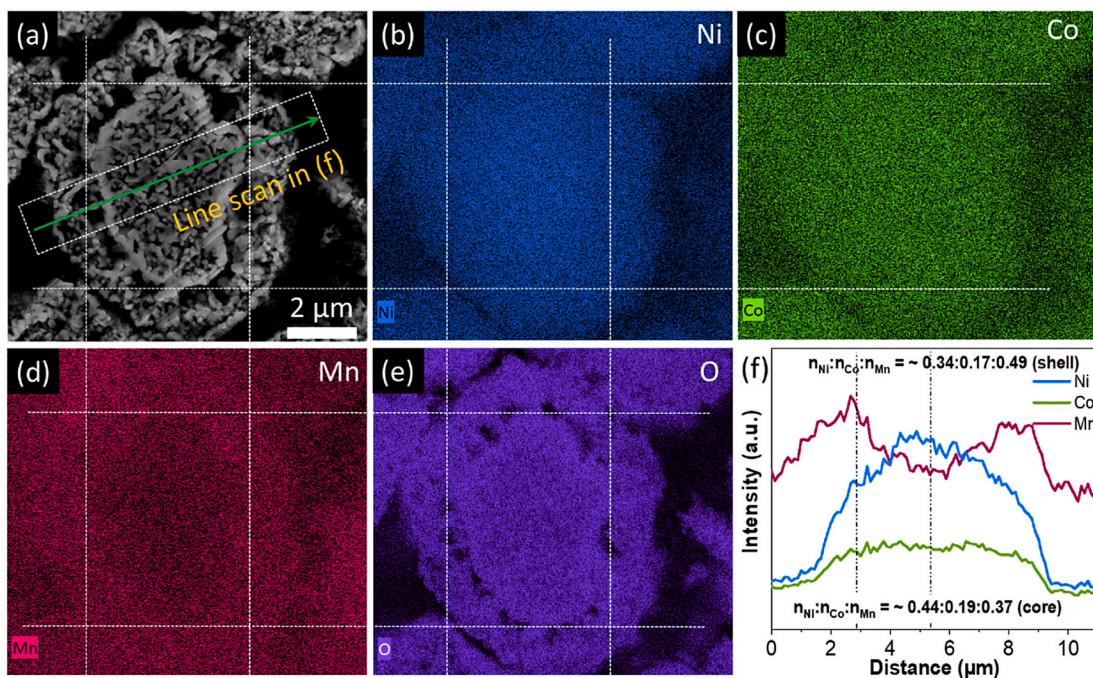


Fig. 1. Core-shell morphology of the prepared NCM material. (a) Cross-sectional SEM image and its corresponding EDX mapping of (b) nickel, (c) cobalt, (d) manganese and (e) oxygen elements of the prepared core-shell NCM material, (f) line-scan EDX intensity profile of the elements as a function of the distance.

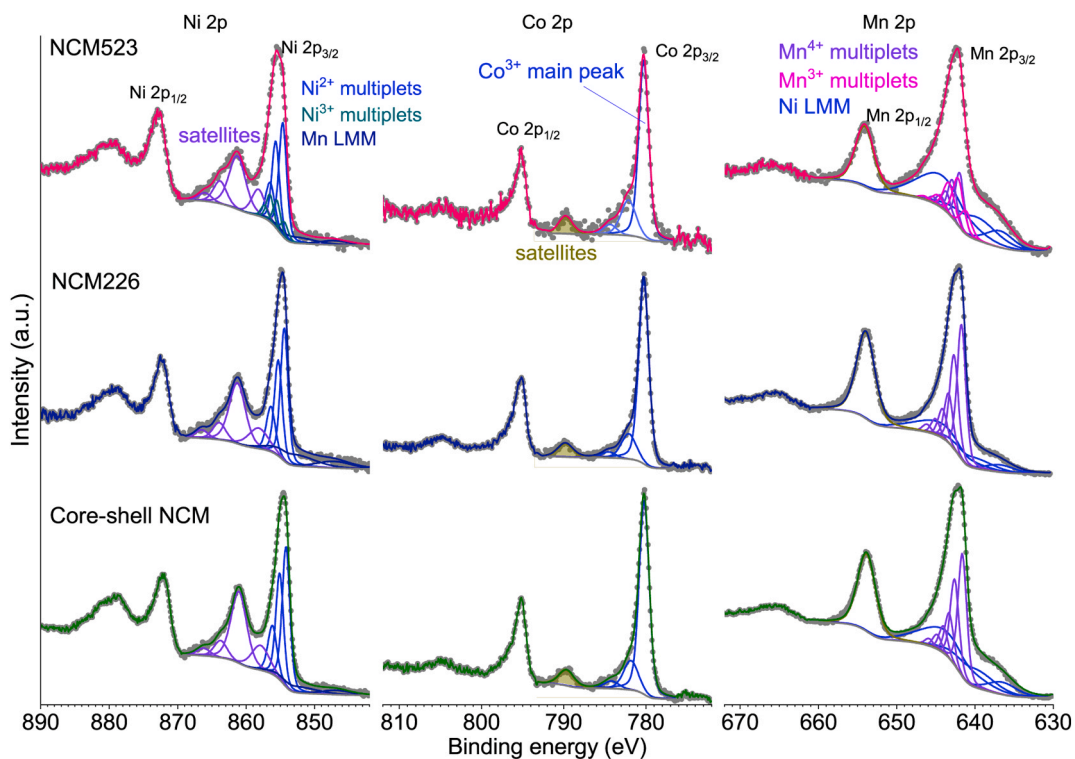


Fig. 2. Ni 2p, Co 2p, and Mn 2p XP spectra of NCM523 (top), NCM226 (middle), core-shell NCM (bottom).

layered phase ( $C2/m$ ) are found in NCM226, which is usually observed in Mn-rich layered oxides [34]. For comparison, Rietveld refinements for both NCM523 and NCM226 were performed by assuming a layered rhombohedral model ( $R\bar{3}m$ ), as shown in Fig. 3(a-b) and Tables S1–2. Considering the neutron powder diffraction (NPD) is sensitive to discriminate the transition metals with similar electronic densities (i.e. Ni, Co and Mn), high-resolution SRD and NPD were combined to

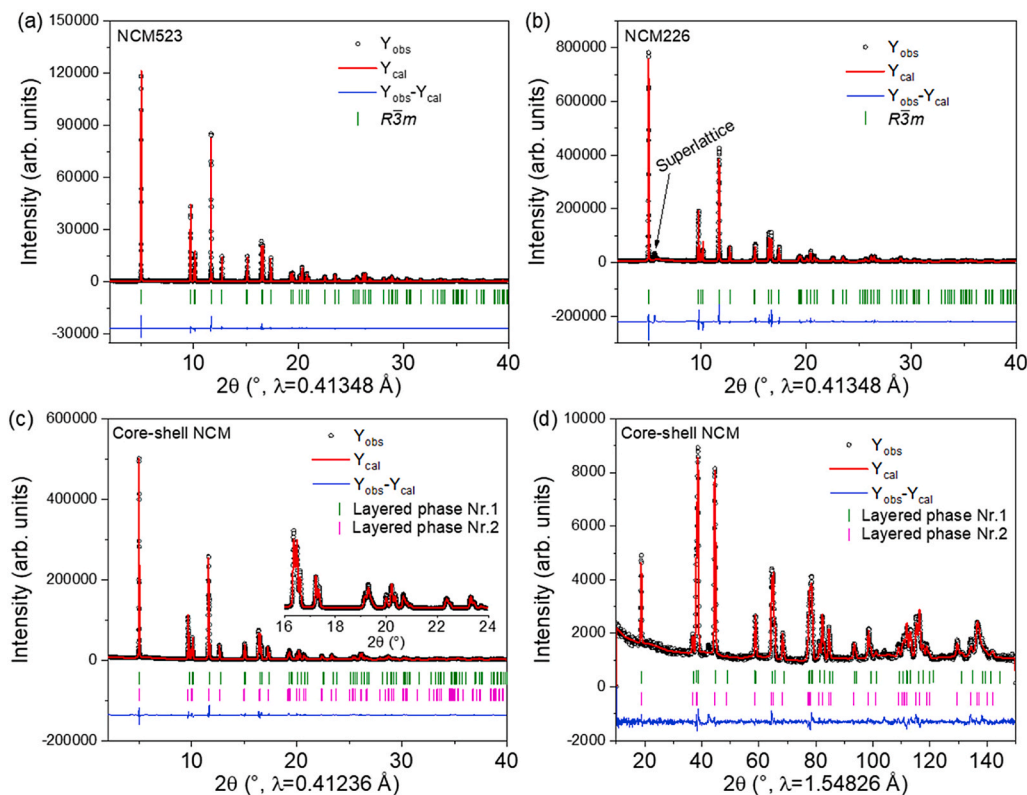
determine the actual structure and to evaluate the chemical composition of prepared core-shell NCM material, see Fig. 3(c-d). Two layered  $\alpha$ - $\text{NaFeO}_2$  structures with the same  $R\bar{3}m$  space group are determined in the sample. The absence of superlattice reflections at around  $5.6^\circ$  excludes the possibility of monoclinic layered phase ( $C2/m$ ) formation, which suggests that the Mn-rich shell may not have the same chemical composition as the NCM226 because of inter-diffusion of Ni and Mn in

**Table 1**

XPS quantification results of the samples.

Item	Ni		Co		Mn	
	Oxidation state	Normalized atomic %	Oxidation state	Normalized atomic %	Oxidation state	Normalized atomic %
NCM532	~80% Ni <sup>2+</sup> ~20% Ni <sup>3+</sup>	0.7	Co <sup>3+</sup>	0.2	~50% Mn <sup>3+</sup> ~50% Mn <sup>4+</sup>	0.2
NCM226	Ni <sup>2+</sup>	0.3	Co <sup>3+</sup>	0.2	Mn <sup>4+</sup>	0.4
Core-Shell NCM	Ni <sup>2+</sup>	0.5	Co <sup>3+</sup>	0.2	Mn <sup>4+</sup>	0.4

Standard deviation: &lt; 10% of atomic concentration, Binding energy uncertainty: ±0.2 eV.

**Fig. 3.** Rietveld refinement against SRD patterns of (a) NCM523 and (b) NCM226; a simultaneous Rietveld refinement against (c) SRD and (d) NPD data of the core-shell NCM material, indicating an existence of two layered phases.

core-shell NCM particles during heating. Simultaneous Rietveld refinement against NPD and SRD results were completed by assuming layered  $\text{LiNi}_{0.5}\text{Co}_{0.2}\text{Mn}_{0.3}\text{O}_2$  (phase Nr.1) and layered  $\text{LiNi}_{0.2}\text{Co}_{0.2}\text{Mn}_{0.6}\text{O}_2$  (phase Nr.2) with the same space group of  $R\bar{3}m$ . A good fit indicates that the structural model is reliable. The lattice parameters of the sample are depicted in Fig. 3 and Table S3, respectively. The layered Ni-rich phase Nr.1 presents an increase of both  $a$  and  $c$  lattice parameters when compared with the Mn-rich layered phase Nr.2, which can be attributed to the larger ionic radius of  $\text{Ni}^{2+}$  with respect to  $\text{Mn}^{4+}$  ions ( $r_{\text{Ni}^{2+}} = 0.69 \text{ \AA}$ ,  $r_{\text{Mn}^{4+}} = 0.53 \text{ \AA}$ ). Even though quantification of the Ni, Co and Mn content along the particles is not straight forward, all the SRD, NPD, XPS and EDX results are consistent with the presence of a layered Ni-rich core surrounded by a layered Mn-rich shell in the obtained material.

To study the electrochemical performance of the prepared cathode materials in LIBs, core-shell NCM, conventional NCM523, and conventional NCM226 were assembled into coin-type cells (CR2032) and tested between 2.7 and 4.3 V against Li metal at a current density of  $27 \text{ mA g}^{-1}$  (0.1 C) at room temperature. The charge and discharge curves of three electrodes (Fig. 4(a)) exhibit a similar smooth and monotonic charge-discharge profile, which is a typical solid-solution-like reaction characteristic of layered NCM materials [35]. As shown in Fig. 4(a), the electrodes exhibit different reaction potentials, probably because of

their various chemical compositions. The initial discharge capacity of the core-shell NCM and the NCM523 was tested to be  $158(5)$  and  $157(5) \text{ mA h g}^{-1}$ , respectively, which is higher than the value of the NCM226 ( $134(5) \text{ mA h g}^{-1}$ ). The differential capacity ( $dQ \text{ dV}^{-1}$ ) curves of the electrodes are shown in Fig. 4(b). Two  $dQ/\text{dV}$  vs.  $V$  (oxidation) peaks are observed upon the first charge of the NCM523 (at around 3.73 and 3.80 V). Only a broad redox peak is found in the core-shell NCM compared to the NCM523 and the NCM226. The number changes in  $dQ \text{ dV}^{-1}$  peaks indicate that the core-shell NCM cannot simply be considered as a physical mixture of layered NCM523 and layered NCM226. The diffusion coefficient of  $\text{Li}^+$  ( $D_{\text{Li}^+}$ ) of the electrodes, obtained by the potentiostatic intermittent titration technique (PITT) (Fig. S10), is shown in Fig. 4(c). The  $D_{\text{Li}^+}$  of the core-shell NCM is close to that of the NCM226 during the initial charge, but is lower than that of the NCM523. Thus, the Li-ion transport from centre to surface of the secondary particles is possibly limited by the surface Mn-rich shell. These data reveal that the core-shell NCM cathode has integrated electrochemical behaviours of the Ni-rich core and the Mn-rich shell phases, i.e. the Mn-rich NCM shell dominates the potential curve at the beginning of charge process and the Ni-rich NCM core material leads to a higher capacity.

Fig. 4(d) shows the cycling stability of core-shell NCM, NCM523, and NCM226 cathodes. It is obvious that the core-shell NCM electrode

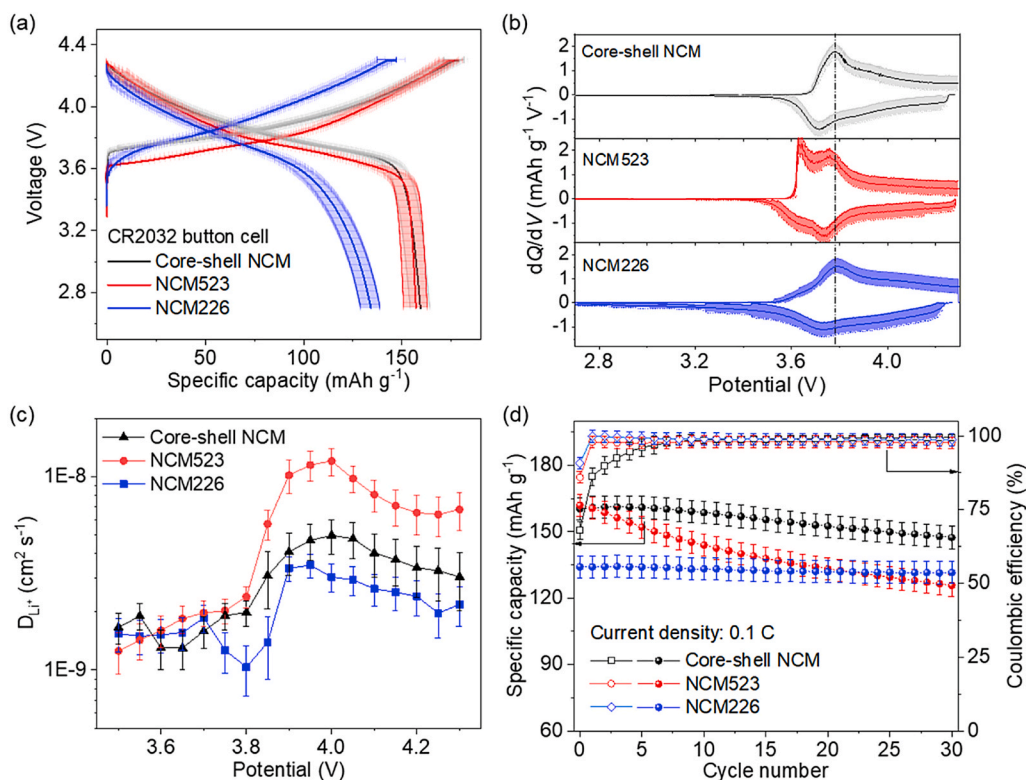


**Fig. 4.** Electrochemical properties of electrodes. (a) The initial charge-discharge voltage plots (b) the corresponding voltage derivatives of the specific capacity vs. voltage, (c) Li-ion diffusion coefficients ( $D_{Li^+}$ ) calculated from the PITT curves vs. potential during the first charge process and (d) cycling performance and the corresponding coulombic efficiency of core-shell NCM, NCM523 and NCM226 electrodes at 0.1C.

displays an improved electrochemical performance with a capacity retention of around 92% after 30 cycles at 0.1 C, when compared with the NCM523 electrode ( $\sim 78\%$ ). The morphology of core-shell NCM is

basically maintained after cycling, as supported by the EDX elemental mapping images in Fig. S11, thereby, favouring the improvement of its cycling stability. By contrast the discharge capacity of NCM226 is 131

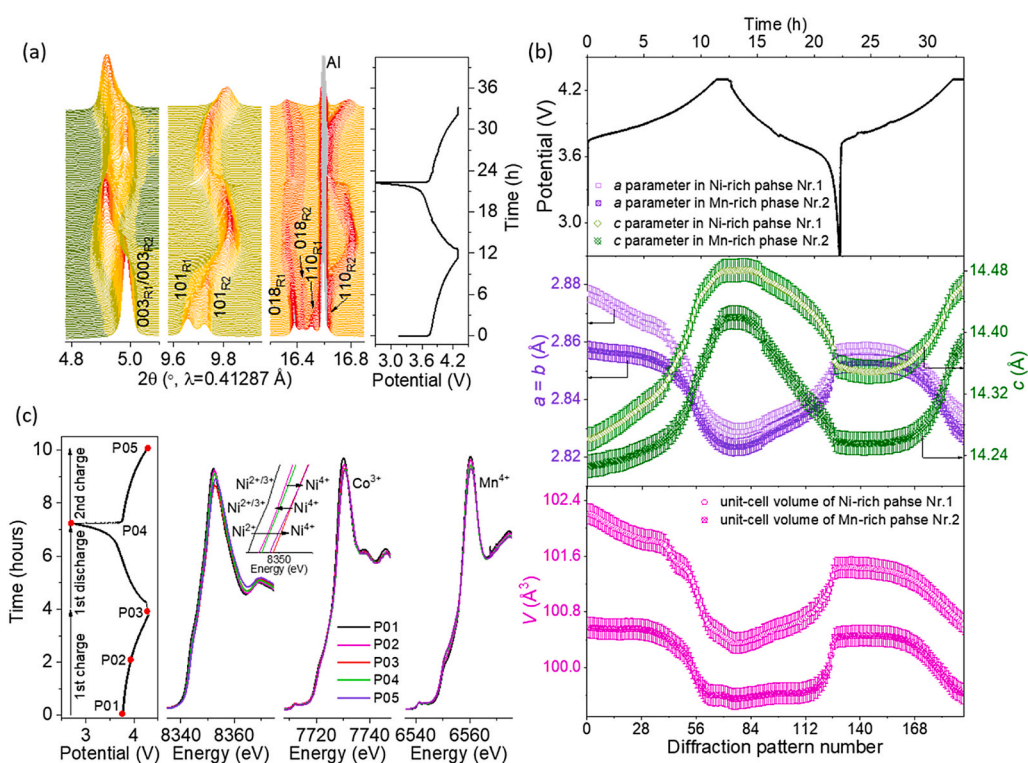


**Fig. 5.** (De)Lithiation mechanism of core-shell NCM cathode materials during cycling. (a) SRD reflection evolution of 003, 101, 018, and 110 of the core-shell NCM electrode during the first charge-discharge and the second charge process in the voltage range from 2.7 to 4.3 V, R1 and R2 represent the rhombohedral Ni-rich layered phase Nr.1 and the rhombohedral Mn-rich layered phase Nr.2, respectively; (b) variation of lattice parameter as a function of delithiation and lithiation process, lattice parameters of each SRD pattern were calculated by using Rietveld refinement with two layered phases ( $R\bar{3}m$ ), revealing a good structural stability for the Mn-rich phase Nr.2; (c) *in situ* XANES spectra at Ni, Co, and Mn K-edges of the core-shell NCM cathode during cycling.

mA h g<sup>-1</sup> after 30 cycles, retaining about 98% of its initial capacity. Interestingly, the core-shell NCM electrode can still deliver a high capacity of ~110 mA h g<sup>-1</sup>, retaining approximately 69% of its initial capacity (~160 mA h g<sup>-1</sup>) after high current density cycling (i.e. from 0.1 C to 20 C), see Fig. S12. However, it is very difficult to discriminate the insertion/extraction behavior of Li-ions into the two individual, but similar, layered phases of the core-shell particles during cycling by electrochemical characterizations, since the shape of the electrochemical profiles agrees well with the results reported for conventional homogenous particles reported in the literature [36–38] and those of the layered NCM electrode (see Fig. 4(a)).

In order to unveil the structural and electronic evolution of the core-shell NCM electrode during electrochemical lithiation/delithiation in the voltage range from 2.7 to 4.3 V, *in situ* SRD and *in situ* X-ray absorption near-edge structure (XANES) experiments were performed, as shown in Fig. 5. During delithiation (charging) process, the 003 reflection gradually moves towards smaller  $2\theta$  angles. This can be ascribed to an increased lattice parameter  $c$  of the unit cell as Li ions extract from the Li layer, leading to an increased electrostatic repulsion between two neighbouring oxygen layers. Meanwhile, the 101 and 110 reflections shift to larger scattering angles demonstrating the decrease in the lattice parameter  $a$  ( $a = b$ ), since TM–O bonds in TMO<sub>6</sub> octahedra are shrinking upon charging. No significant change in the Co K-edge and Mn K-edge spectra are observed, see Fig. 5(c). The valence state of Co, and Mn looks not to change significantly as a function of reaction time and can be assigned close to 3+, and 4+, respectively. The Ni K-edge absorption rising edge shifts slightly towards higher energy by charging suggesting a structural contraction involving the Ni sites. Most likely the detected contraction in the  $a$ - $b$  plane is principally involving Ni–O atomic pairs. The changes of lattice parameters show a reverse direction during the lithiation process, but both the Ni-rich phase (layered phase Nr.1) and the Mn-rich phase (layered phase Nr.2) phases do not return to their pristine state, especially for Ni-rich phase Nr.1, see (Fig. 5(a-b)). It looks like that the first charge is partially irreversible, differently for the next cycles.

Very impressively, the lattice parameters (i.e.  $a$ ,  $c$  and  $V$ ) of the Ni-rich phase (layered phase Nr.1) change dramatically at the beginning of charge when compared with those of the Mn-rich phase (layered phase Nr.2), see Fig. 5(b). This small lattice parameter changes of the Mn-rich shell may have resulted from a relatively high Li-ion concentration since the Li-ion extracted from the Ni-rich core needs to pass through the Mn-rich shell. During the first discharge, the insertion of Li-ion into the Ni-rich phase is found to be slightly later when compared with the Mn-rich phase, as evidenced by a slow decrease in the lattice parameter  $c$  of layered phase Nr.1. It is worth to point out that both the Ni-rich phase and the Mn-rich phase reveal a similar ‘unit cell breathing’ mechanism during the first cycle [34], but both phases do not return to their pristine state, especially for Ni-rich phase Nr.1, see Fig. 5(a and b). This is probably due to the fact that the lithium-ion intercalation into the core-shell NCM stops before the core material is fully discharged, see *in situ* XANES spectra in Fig. 5(c). After the first cycle between 2.7 V and 4.3 V, the changes in the parameter  $a$ ,  $c$  and the unit cell volume  $V$  of the Ni-rich phase Nr.1 are 0.69, 0.62 and 0.76%, respectively, which are higher than that of the Mn-rich phase Nr.2 (0.16, 0.21 and 0.11%). Since the transition metal oxidation states seem not to change considerably, it is possible to assume that the reported structural variation are purely coming from the Li removal and consequent increase of the interlayer repulsion, with the Ni–O bonds being initially more flexible than those of the Mn–O. These results suggest the Ni-rich layered phase to enhance at least the first cycle capacity [39,40], with the Mn-rich exterior phase providing a protection layer for improving the structural stability. During the second charging process, the evolution of the lattice parameters for both phases is nearly synchronous, suggesting that the defective Ni-rich core exhibits a similar electrochemical behavior as the Mn-rich shell.

To further elucidate the Li-ion (de)intercalation process for core-

shell NCM, a comparison study of *in situ* X-Ray powder diffraction (XRD) measurements of NCM532 and NCM226 electrodes was carried out, as shown in Fig. 6. Continuous changes of positions of reflections in the *in situ* diffraction patterns of both electrodes indicate a solid-solution reaction mechanism upon cycling (Fig. 6(a) and (c)). The variation of corresponding lattice parameters,  $a$ ,  $c$  and  $V$ , are displayed in Fig. 6(b) and (d). Evidently, in contrast to NCM523, NCM226 has less pronounced alteration of lattice parameters, which could mitigate the mechanical and structural degradation and thus lead to a good cycling performance (Fig. 4(d)). Noticeably, the changes in the parameter  $a$ ,  $c$  and  $V$  of the NCM523 are 0.20(2), –0.41(2) and –0.01(1) %, respectively, which is smaller than those of the Ni-rich phase Nr.1 in the core-shell NCM (see above). From the result above, a subsequent (de)lithiation process in the core-shell NCM electrode during the first cycle is proposed, as shown in Fig. 7. Due to the fact that the core-shell NCM material has fine open pores (Fig. 1(a)), lithium ions are firstly extracted from the Ni-rich core phase because of its higher concentration of reactive Ni, see *in situ* SRD results in Fig. 5(b). Since the  $D_{Li^+}$  of Mn-rich phase is lower than that of the Ni-rich phase during the initial charge (Fig. 4(c)), the state of charge of the shell thus determines the electrochemical characteristics of the core-shell NCM and leads to the disappearance of the first peak at ~ 3.6 V in the dQ/dV curve of the NCM523 (Fig. 4(b)). This means that, at the end of charging, the Ni-rich core experiences a larger variation of lattice parameters compared to the Mn-rich shell (less Li-ion vacancies). During the first discharge, lithium ions have to diffuse through the Mn-rich shell with a poor kinetic behavior, which makes them difficult to intercalate into the Ni-rich core, see Figs. 5(b) and Figure 6(b). Therefore, an irreversible part of the structural evolution detected in the first charge is most likely caused by an irreversible lithium loss, resulting in a low columbic efficiency (Fig. 4(d)) and the formation of Li-deficient Ni-rich core (Fig. 7). While the partially irreversible change in the core-shell architecture during the initial cycle does not affect the final functional properties dramatically, see Fig. 4(d).

### 3. Conclusion

In summary, a core-shell NCM material was successfully synthesized by a hydroxide co-precipitation method followed by sintering with Li<sub>2</sub>CO<sub>3</sub>. Simultaneous Rietveld refinement against high-resolution SRD and NPD data reveals that the prepared core-shell NCM material consists of two similar layered rhombohedral phases ( $R\bar{3}m$ ), an inner Ni-rich core and a Mn-rich shell (on a secondary particle level). The Ni-rich phase appears to contribute more to the initial capacity, while the Mn-rich phase is supposed to be beneficial for the cathode structural stability. These findings could offer an intriguing explanation for the synergistic effect of the two layered phases in the core-shell morphology on the electrochemical performance of NCM cathode materials. Currently, the facile synthetic route is being utilized to synthesize Co-free Ni-rich layered NCM cathode materials with core-shell architecture in our group. Therefore, preparation procedure might be helpful for synthesizing the core-shell or concentration gradient oxide-based cathode materials for Li/Na ion batteries with good performance by structural design, morphological regulation, and chemical composition optimization.

### CRedit authorship contribution statement

**Weibo Hua:** The experimental data were measured and analysed by. **Björn Schwarz:** conceived the idea and oversaw the project, interpreted and discussed the data, wrote the article, The experimental data were measured and analysed by. **Raheleh Azmi:** interpreted and discussed the data, The experimental data were measured and analysed by. **Marcus Müller:** The experimental data were measured and analysed by. **Mariyam Susana Dewi Darma:** The experimental data were measured and analysed by. **Michael Knapp:** interpreted and discussed the data.

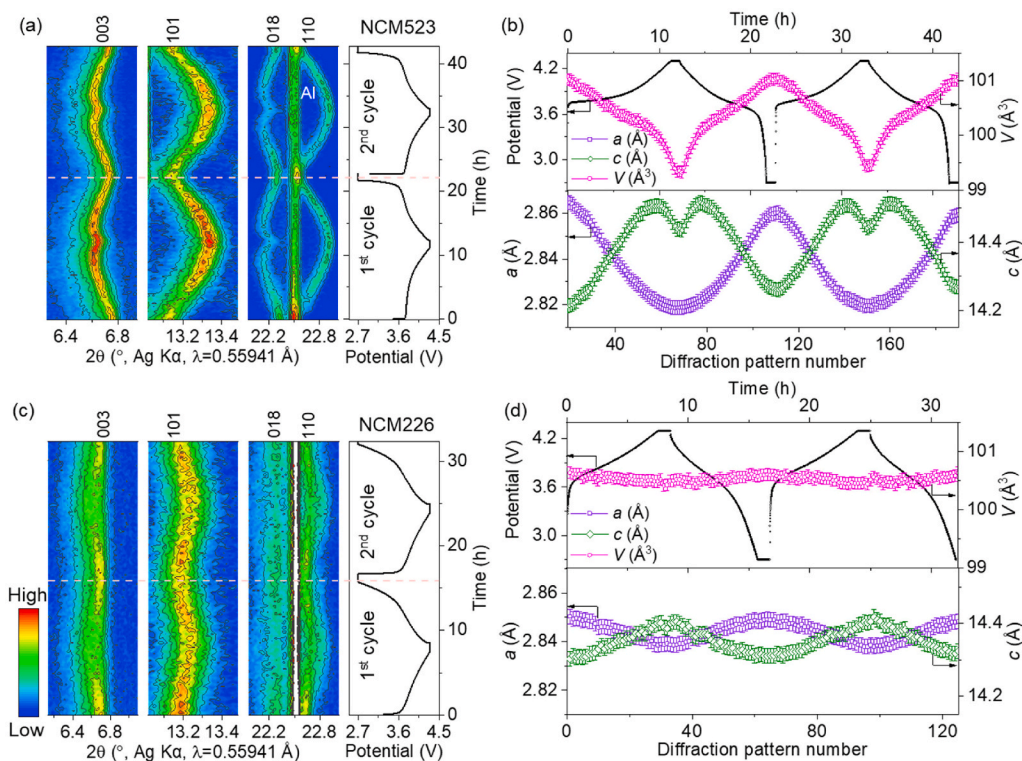


**Fig. 6.** (De)Lithiation mechanism of NCM523 and NCM226 during cycling. XRD reflection evolution of 003, 101, 018, and 110 of (a) NCM523 and (c) NCM226 electrodes during the first two cycles between 2.7 and 4.3 V; (b) variation of lattice parameter as a function of de-lithiation and lithiation process for (b) NCM523 and (d) NCM226 electrodes.

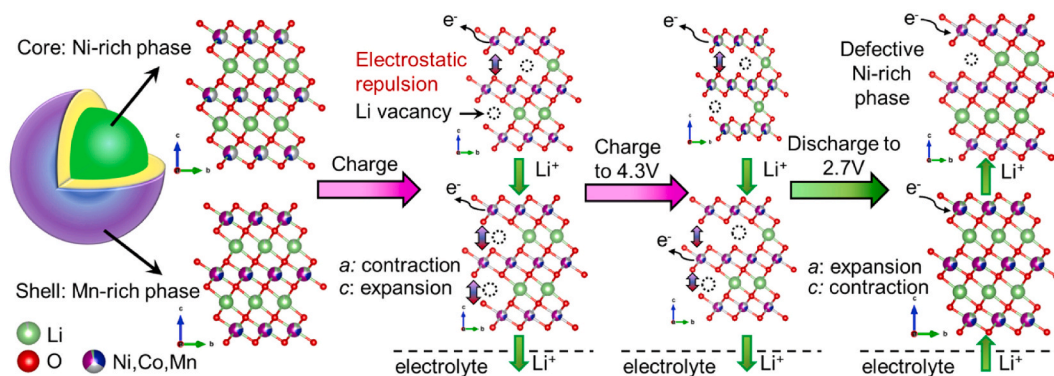


**Fig. 7.** Schematic illustration of a subsequent (de)lithiation mechanism in the core-shell NCM cathode materials during the first cycle, showing an obvious change in the unit-cell volume of the Ni-rich phase within the interior region of a secondary particle with respect to the Mn-rich phase. TM: Ni – whitish; Mn – magenta; Co – blue.

wrote the article. **Anatoliy Senyshyn:** R.Z, The experimental data were measured and analysed by. **Michael Heere:** The experimental data were measured and analysed by. **Alkesandr Missiul:** The experimental data were measured and analysed by. **Laura Simonelli:** The experimental data were measured and analysed by. **Joachim R. Binder:** interpreted and discussed the data. **Sylvio Indris:** interpreted and discussed the data, The experimental data were measured and analysed by. **Helmut Ehrenberg:** interpreted and discussed the data. wrote the article.

#### Declaration of competing interest

The authors declare that they have no known competing financial interests or personal relationships that could have appeared to influence the work reported in this paper.

#### Acknowledgements

W.H. received financial support from the Helmholtz – OCPC Postdoc-Program. The Bundesministerium für Bildung und Forschung (BMBF) supported Energy Research with Neutrons (ErWiN) with Grant No. 05K16VK2/05K19VK3. Part of these experiments were performed at the MSPD beamline and the CLAESS beamline at ALBA Synchrotron with the collaboration of ALBA staff. The authors gratefully acknowledge Margarete Offermann for helping with the particle size distribution measurements and Udo Geckle for the SEM-EDX experiments. This work contributes to the research performed at CELEST (Center for Electrochemical Energy Storage Ulm-Karlsruhe).

## Appendix A. Supplementary data

Supplementary data to this article can be found online at <https://doi.org/10.1016/j.nanoen.2020.105231>.

## References

- X. Wu, S. Yao, Flexible electrode materials based on WO<sub>3</sub> nanotube bundles for high performance energy storage devices, *Nano Energy* 42 (2017) 143–150, <https://doi.org/10.1016/j.nanoen.2017.10.058>.
- D. Zhao, M. Dai, H. Liu, L. Xiao, X. Wu, H. Xia, Constructing high performance hybrid battery and electrocatalyst by heterostructured NiCo<sub>2</sub>O<sub>4</sub>@NiWS nanosheets, *Cryst. Growth Des.* 19 (3) (2019) 1921–1929, <https://doi.org/10.1021/acs.cgd.8b01904>.
- D. Zhao, H. Liu, X. Wu, Bi-interface induced multi-active MC<sub>2</sub>O<sub>4</sub>@MC<sub>2</sub>O<sub>4</sub>/PPy (M=Ni, Zn) sandwich structure for energy storage and electrocatalysis, *Nano Energy* 57 (2019) 363–370, <https://doi.org/10.1016/j.nanoen.2018.12.066>.
- D. Chen, H. Tan, X. Rui, Q. Zhang, Y. Feng, H. Geng, C. Li, S. Huang, Y. Yu, Oxivanite V<sub>2</sub>O<sub>5</sub>: a new intercalation-type anode for lithium-ion battery, *InfoMat* 1 (2) (2019) 251–259, <https://doi.org/10.1002/inf2.12011>.
- Z. Liu, Q. Yu, Y. Zhao, R. He, M. Xu, S. Feng, S. Li, L. Zhou, L. Mai, Silicon oxides: a promising family of anode materials for lithium-ion batteries, *Chem. Soc. Rev.* 48 (1) (2019) 285–309, <https://doi.org/10.1039/c8cs00441b>.
- Z. Liu, D. Guan, Q. Yu, L. Xu, Z. Zhuang, T. Zhu, D. Zhao, L. Zhou, L. Mai, Monodisperse and homogeneous SiO<sub>x</sub>/C microspheres: a promising high-capacity and durable anode material for lithium-ion batteries, *Energy Storage Mater.* 13 (2018) 112–118, <https://doi.org/10.1016/j.ensm.2018.01.004>.
- D. Zhao, M. Dai, Y. Zhao, H. Liu, Y. Liu, X. Wu, Improving electrocatalytic activities of FeCo<sub>2</sub>O<sub>4</sub>@FeCo<sub>2</sub>S<sub>4</sub>/PPy electrodes by surface/interface regulation, *Nano Energy* 72 (2020), <https://doi.org/10.1016/j.nanoen.2020.104715>, 104715.
- C. Liu, X. Wu, B. Wang, Performance modulation of energy storage devices: a case of Ni-Co-S electrode materials, *Chem. Eng. J.* 392 (2020), <https://doi.org/10.1016/j.cej.2019.123651>, 123651.
- L. Grande, E. Paillard, J. Hassoun, J.B. Park, Y.J. Lee, Y.K. Sun, S. Passerini, B. Scrosati, The lithium/air battery: still an emerging system or a practical reality? *Adv. Mater.* 27 (5) (2014) 784–800, <https://doi.org/10.1002/adma.201403064>.
- Y. Qiao, J. Yi, S. Wu, Y. Liu, S. Yang, P. He, H. Zhou, Li-CO<sub>2</sub> Electrochemistry: a new strategy for CO<sub>2</sub> fixation and energy storage, *Joule* 1 (2017) 359–370, <https://doi.org/10.1016/j.joule.2017.07.001>.
- P. Bai, M.Z. Bazant, Charge transfer kinetics at the solid-solid interface in porous electrodes, *Nat. Commun.* 5 (2014), <https://doi.org/10.1038/ncomms4585>, 3585.
- X. Zhang, M. Van Hulzen, D.P. Singh, A. Brownrigg, J.P. Wright, N.H. Van Dijk, M. Wagemaker, Direct view on the phase evolution in individual LiFePO<sub>4</sub> nanoparticles during Li-ion battery cycling, *Nat. Commun.* 6 (2015) 1–7, <https://doi.org/10.1038/ncomms9333>.
- G.L. Xu, Q. Liu, K.K.S. Lau, Y. Liu, X. Liu, H. Gao, X. Zhou, M. Zhuang, Y. Ren, J. Li, M. Shao, M. Ouyang, F. Pan, Z. Chen, K. Amine, G. Chen, Building ultraconformal protective layers on both secondary and primary particles of layered lithium transition metal oxide cathodes, *Nat. Energy* 4 (6) (2019) 484–494, <https://doi.org/10.1038/s41560-019-0387-1>.
- Y. Wei, J. Zheng, S. Cui, X. Song, Y. Su, W. Deng, Z. Wu, X. Wang, W. Wang, M. Rao, Y. Lin, C. Wang, K. Amine, F. Pan, Kinetics tuning of Li-ion diffusion in layered Li(Ni<sub>x</sub>Mn<sub>y</sub>Co<sub>z</sub>)O<sub>2</sub>, *J. Am. Chem. Soc.* 137 (2015) 8364–8367, <https://doi.org/10.1021/jacs.5b04040>.
- W. Hua, M. Chen, B. Schwarz, M. Knapp, M. Bruns, J. Barthel, X. Yang, F. Sigel, R. Azmi, A. Senyshyn, A. Missiul, L. Simonelli, M. Etter, S. Wang, X. Mu, A. Fiedler, J.R. Binder, X. Guo, S. Chou, B. Zhong, S. Indris, H. Ehrenberg, Lithium/oxygen incorporation and microstructural evolution during synthesis of Li-rich layered Li [Li<sub>0.2</sub>Ni<sub>0.2</sub>Mn<sub>0.6</sub>]O<sub>2</sub> oxides, *Adv. Energy Mater.* 8 (2019), <https://doi.org/10.1002/aenm.201803094>, 1803094.
- S. Bae, H.D. Song, I. Nam, G.P. Kim, J.M. Lee, J. Yi, Quantitative performance analysis of graphite-LiFePO<sub>4</sub> battery working at low temperature, *Chem. Eng. Sci.* 118 (2014) 74–82, <https://doi.org/10.1016/j.ces.2014.07.042>.
- X. Mu, A. Kober, D. Wang, V.S.K. Chakravadhanula, S. Schlabach, D.V. Szabó, P. Norby, C. Kübel, Comprehensive analysis of TEM methods for LiFePO<sub>4</sub>/FePO<sub>4</sub> phase mapping: spectroscopic techniques (EFTEM, STEM-EELS) and STEM diffraction techniques (ACOM-TEM), *Ultramicroscopy* 170 (2016) 10–18, <https://doi.org/10.1016/j.ultramic.2016.07.009>.
- Y. Li, F. El Gabaly, T.R. Ferguson, R.B. Smith, N.C. Bartelt, J.D. Sugar, K.R. Fenton, D.A. Cogswell, A.L.D. Kilcoyne, T. Tylliszczak, M.Z. Bazant, W.C. Chueh, Current-induced transition from particle-by-particle to concurrent intercalation in phase-separating battery electrodes, *Nat. Mater.* 13 (2014) 1149–1156, <https://doi.org/10.1038/nmat4084>.
- L. de Biasi, B. Schwarz, T. Brezesinski, P. Hartmann, J. Janek, H. Ehrenberg, Chemical, structural, and electronic aspects of formation and degradation behavior on different length scales of Ni-rich NCM and Li-rich HE-NCM cathode materials in Li-ion batteries, *Adv. Mater.* 31 (26) (2019), <https://doi.org/10.1002/adma.201900985>, 1900985.
- U.-H. Kim, D.-W. Jun, K.-J. Park, Q. Zhang, P. Kaghazchi, D. Aurbach, D.T. Major, G. Goebes, M. Dixit, N. Leifer, C.M. Wang, P. Yan, D. Ahn, K.-H. Kim, C.S. Yoon, Y.-K. Sun, Pushing the limit of layered transition metal oxide cathodes for high-energy density rechargeable Li ion batteries, *Energy Environ. Sci.* 11 (5) (2018) 1271–1279, <https://doi.org/10.1039/C8EE00227D>.
- D. Wang, R. Kou, Y. Ren, C.J. Sun, H. Zhao, M.J. Zhang, Y. Li, A. Huq, J.Y.P. Ko, F. Pan, Y.K. Sun, Y. Yang, K. Amine, J. Bai, Z. Chen, F. Wang, Synthetic control of kinetic reaction pathway and cationic ordering in high-Ni layered oxide cathodes, *Adv. Mater.* 29 (39) (2017) 1606715, <https://doi.org/10.1002/adma.201606715>.
- W. Zhang, D.H. Seo, T. Chen, L. Wu, M. Tropsakal, Y. Zhu, D. Lu, G. Ceder, F. Wang, Kinetic pathways of ionic transport in fast-charging lithium titanate, *Science* 367 (6481) (2020) 1030–1034, <https://doi.org/10.1126/science.aax3520>.
- D.-W. Jun, C.S. Yoon, U.-H. Kim, Y.-K. Sun, High-energy density core-shell structured Li[Ni<sub>0.95</sub>Co<sub>0.025</sub>Mn<sub>0.025</sub>]O<sub>2</sub> cathode for lithium-ion batteries, *Chem. Mater.* 29 (2017) 5048–5052, <https://doi.org/10.1021/acs.chemmater.7b01425>.
- S.-K. Jung, H. Gwon, J. Hong, K.-Y. Park, D.-H. Seo, H. Kim, J. Hyun, W. Yang, K. Kang, Understanding the degradation mechanisms of LiNi<sub>0.5</sub>Co<sub>0.2</sub>Mn<sub>0.3</sub>O<sub>2</sub> cathode material in lithium ion batteries, *Adv. Energy Mater.* 4 (1) (2013), <https://doi.org/10.1002/aenm.201300787>, 1300787.
- A.K. Shukla, Q. Ramasse, C. Ophus, D.M. Kepaptsoglou, F.S. Hage, C. Gammer, C. Bowling, P.A.H.-andez Gallegos, S. Venkatachalam, Effect of composition on the structure of lithium- and manganese-rich transition metal oxides, *Energy Environ. Sci.* 11 (4) (2018) 830–840, <https://doi.org/10.1039/C7EE02443F>.
- Y.-K. Sun, Z. Chen, H.-J. Noh, D.-J. Lee, H.-G. Jung, Y. Ren, S. Wang, C.S. Yoon, S.-T. Myung, K. Amine, Nanostructured high-energy cathode materials for advanced lithium batteries, *Nat. Mater.* 11 (2012) 942–947, <https://doi.org/10.1038/nmat3435>.
- Y.-K. Sun, S.-T. Myung, M.-H. Kim, J. Prakash, K. Amine, Synthesis and characterization of Li[(Ni<sub>0.8</sub>Co<sub>0.1</sub>Mn<sub>0.1</sub>)<sub>0.8</sub>(Ni<sub>0.5</sub>Mn<sub>0.5</sub>)<sub>0.2</sub>]O<sub>2</sub> with the microscale core-shell structure as the positive electrode material for lithium batteries, *J. Am. Chem. Soc.* 127 (2005) 13411–13418, <https://doi.org/10.1021/ja053675g>.
- W. Hua, Z. Wu, M. Chen, M. Knapp, X. Guo, S. Indris, J.R. Binder, N.N. Bramnik, B. Zhong, H. Guo, S. Chou, Y.-M. Kang, H. Ehrenberg, Shape-controlled synthesis of hierarchically layered lithium transition-metal oxide cathode materials by shear exfoliation in continuous stirred-tank reactors, *J. Mater. Chem. A* 5 (2017) 25391–25400, <https://doi.org/10.1039/C7TA08073E>.
- W. Hua, W. Liu, M. Chen, S. Indris, Z. Zheng, X. Guo, M. Bruns, T.-H. Wu, Y. Chen, B. Zhong, S. Chou, Y.-M. Kang, H. Ehrenberg, Unravelling the growth mechanism of hierarchically structured Ni<sub>1/3</sub>Co<sub>1/3</sub>Mn<sub>1/3</sub>(OH)<sub>2</sub> and their application as precursors for high-power cathode materials, *Electrochim. Acta* 232 (2017) 123–131, <https://doi.org/10.1016/j.electacta.2017.02.105>.
- W.B. Hua, X.D. Guo, Z. Zheng, Y.J. Wang, B.H. Zhong, B. Fang, J.Z. Wang, S. L. Chou, H. Liu, Uncovering a facile large-scale synthesis of LiNi<sub>1/3</sub>Co<sub>1/3</sub>Mn<sub>1/3</sub>O<sub>2</sub> nanoflowers for high power lithium-ion batteries, *J. Power Sources* 275 (2015) 200–206, <https://doi.org/10.1016/j.jpowsour.2014.09.178>.
- W. Hua, K. Wang, M. Knapp, B. Schwarz, S. Wang, H. Liu, J. Lai, M. Müller, A. Schökel, A. Missyul, D. Ferreira Sanchez, X. Guo, J. Binder, J. Xiong, S. Indris, H. Ehrenberg, Chemical and structural evolution during synthesis of layered Li(Ni, Co, Mn)O<sub>2</sub> oxides, *Chem. Mater.* (2020), <https://doi.org/10.1021/acs.chemmater.9b05279>.
- R. Azmi, M. Masoumi, H. Ehrenberg, V. Trouillet, M. Bruns, Surface analytical characterization of LiNi<sub>0.8-y</sub>Mn<sub>y</sub>Co<sub>0.2</sub>O<sub>2</sub> (0 ≤ y ≤ 0.4) compounds for lithium-ion battery electrodes, *Surf. Interface Anal.* 50 (11) (2018) 1132–1137, <https://doi.org/10.1002/sia.6415>.
- R. Azmi, V. Trouillet, M. Strafela, S. Ulrich, H. Ehrenberg, M. Bruns, Surface analytical approaches to reliably characterize lithium ion battery electrodes, *Surf. Interface Anal.* 50 (1) (2018) 43–51, <https://doi.org/10.1002/sia.6330>.
- W. Hua, S. Wang, M. Knapp, S.J. Leake, A. Senyshyn, M. Yavuz, J.R. Binder, C. P. Grey, H. Ehrenberg, S. Indris, B. Schwarz, Structural insights into the formation and voltage degradation of lithium- and manganese-rich layered oxides, *Nat. Commun.* 10 (2019), <https://doi.org/10.1038/s41467-019-13240-z>, 5365.
- J.B. Goodenough, K.S. Park, The Li-ion rechargeable battery: a perspective, *J. Am. Chem. Soc.* 135 (2013) 1167–1176, <https://doi.org/10.1021/ja3091438>.
- N. Kiziltas-Yavuz, M. Yavuz, S. Indris, N.N. Bramnik, M. Knapp, O. Dolotko, B. Das, H. Ehrenberg, A. Bhaskar, Enhancement of electrochemical performance by simultaneous substitution of Ni and Mn with Fe in Ni-Mn spinel cathodes for Li-ion batteries, *J. Power Sources* 327 (2016) 507–518, <https://doi.org/10.1016/j.jpowsour.2016.07.047>.
- F. Lin, I.M. Markus, D. Nordlund, T.-C. Weng, M.D. Asta, H.L. Xin, M.M. Doeff, Surface reconstruction and chemical evolution of stoichiometric layered cathode materials for lithium-ion batteries, *Nat. Commun.* 5 (2014), <https://doi.org/10.1038/ncomms4529>, 3529.
- C.O. Ehi-eromosele, S. Indris, N.N. Bramnik, A. Sarapulova, V. Trouillet, L. Pfa, G. Melinte, S. Mangold, M. Susana, D. Darma, M. Knapp, H. Ehrenberg, In situ X-ray diffraction and X-ray absorption spectroscopic studies of a lithium-rich layered positive electrode material, *Comp. Compos. Core – Shell Struct.* 12 (12) (2020) 13852–13868, <https://doi.org/10.1021/acsami.9b21061>.
- W. Olszewski, I. Isturiz, C. Marini, M. Avila, M. Okubo, H. Li, H. Zhou, T. Mizokawa, N.L. Saini, L. Simonelli, Effects of nanostructuring on the bond strength and disorder in V<sub>2</sub>O<sub>5</sub> cathode material for rechargeable ion-batteries, *Phys. Chem. Chem. Phys.* 20 (22) (2018) 15288–15292, <https://doi.org/10.1039/c8cp00716k>.
- W. Olszewski, M. Ávila Pérez, C. Marini, E. Paris, X. Wang, T. Iwao, M. Okubo, A. Yamada, T. Mizokawa, N.L. Saini, L. Simonelli, Temperature dependent local structure of Na<sub>x</sub>CoO<sub>2</sub> cathode material for rechargeable sodium-ion batteries, *J. Phys. Chem. C* 120 (8) (2016) 4227–4232, <https://doi.org/10.1021/acs.jpcc.5b10885>.
- Zeng Ziqi, et al., Enabling an intrinsically safe and high-energy-density 4.5 V-class Li-ion battery with nonflammable electrolyte, *InfoMat* 2 (2020) 984–992, <https://doi.org/10.1002/inf2.12089>.



**Dr. Weibo Hua** is currently a postdoctoral fellow at Karlsruhe Institute of Technology (KIT, Germany) and University of Electronic Science and Technology of China (UESCT). He received his Ph.D. (2019) in Chemistry from KIT and his M.S. (2015) in Chemical Technique from Sichuan University (China). His research interests focus on the scale-up of synthesis methods, the development of advanced electrode materials, especially Li- and Mn-rich / Ni-rich layered oxide cathodes for Li-ion batteries, and the comprehensive understanding of the intrinsic correlation between the preparation, structure, and performance in these materials.



**Dr. Michael Knapp** studied Physics in Heidelberg and Darmstadt (Germany) and did his Doctorate in Materials Science at the TU Darmstadt. For many years he was beamline scientist at the Powder Diffraction Beamline at HASYLAB in Hamburg (Germany) and later on moved to Synchrotron ALBA in Barcelona (Spain) where he was Section Head Materials Science and in charge for the implementation of the MSPD beamline. Today he is deputy Director of IAM-ESS at KIT in Karlsruhe (Germany) and Section head 'Development of Scattering Techniques'.



**Dr. Björn Schwarz** received his Ph.D. degree in Materials Science in 2007 from Technische Universität Darmstadt, Germany. He then served as a post-doctoral research associate from 2007 to 2012 at the Leibniz Institute for Solid State and Materials Research Dresden, Germany, with main research activities on physical/magnetic characterization of transition metal oxides and phase separated metallic glasses. Since 2012 he is scientist at the Institute for Applied Materials – Energy Storage Systems at Karlsruhe Institute of Technology, Germany. His current research interests include the relation between atomic/electronic structure and physical properties/electrochemical reaction mechanisms in various kinds of energy storage materials.



**Dr. Anatoliy Senyshyn** is graduated from Lviv Polytechnic National University (Ukraine). He received his PhD in Solid State Physics in 2004. From 2005 Anatoliy Senyshyn is working at research reactor FRM II - Heinz Maier-Leibnitz Zentrum (MLZ) in Garching (Munich), Germany, where he is responsible for high-resolution diffractometer SPODI and he is coordinator of the MLZ Science Group "Structure Research". One of the major research topics of Anatoliy Senyshyn is the structure of energy materials and electrochemical energy storage systems studied using diffraction of X-rays or neutrons.



**Dr. Raheleh Azmi** is currently a post-doctoral researcher at Karlsruhe Institute of Technology (KIT), Germany. She received her M.Sc. (2014) in Metallurgical Engineering from RWTH Aachen University in Germany and her Ph.D. (2018) in Materials Engineering from KIT. Her current research interests include studying surface and interfaces of energy materials with a particular focus in characterization by surface analytical methods such as XPS and ToF-SIMS.



**Dr. Michael Heere** studied Mechanical Engineering at the Helmut-Schmidt-University in Hamburg, Germany. His PhD in physics was based within the MSCA ITN "ECOSTORE" at the Institute for Energy Technology (IFE) and the University of Oslo, Norway. Now working at the Karlsruhe Institute of Technology (KIT) energy materials as well as diffraction and scattering methods are his forte. Among others, metal hydrides are a special interest for applications such as hydrogen storage and batteries. He is responsible for building a neutron powder diffractometer 'Erwin' (Energy research with Neutrons) at the Research Neutron Source Heinz Maier-Leibnitz Zentrum in Garching (Munich), Germany.



**Dr. Marcus Müller** is a chemist and received his Ph.D. in technical chemistry from the University of Karlsruhe for investigations on carbon fiber-reinforced carbon. After a post-doctoral stay at research center Jülich at the former institute for materials and processes in energy systems, he joined KIT to work on the processing of ceramic microsystems. Since 2012, his research field is on electrochemical energy storage systems. He is primarily investigating electrode-processing effects on cell performance for LIB and post-lithium systems with an emphasis on characterization of battery materials via electron microscopy.



**Dr. Alexander Missyul** is a postdoctoral research associate at ALBA synchrotron light source, Spain. He received his M.S. (2005) in chemistry and Ph.D. (2008) in physical chemistry from St. Petersburg State University, Russia. His research interests focus on *in situ* investigation of the chemical transformations in the solid-state materials by means of the powder X-ray diffraction with a particular emphasis on battery materials and metal-organic frameworks.



**Dr. Mariyam Susana Dewi Darma** is currently a research scientist at the Helmholtz Institute Ulm (HIU)-Electrochemical Energy Storage, Germany. She has investigated degradation mechanisms of various type of commercial Li-ion batteries through post-mortem analysis since 2012, employing various techniques including *in-situ* X-ray Diffraction and electrochemical cycling. Expanding her research interest, she started collaboration in the field of battery modelling since 2018, to shed more light into cell performance under different stress factors.



**Dr. Laura Simonelli** is the CL<sub>2</sub>ESS (Core Level Absorption and Emission spectroscopy) beamline responsible at the ALBA light source (Barcelona, Spain). Her research activities are focused on the investigation of functional materials (highly correlated systems including battery materials, high- $T_c$  superconductors, and environments or health correlated materials), with particular interest into the study of the interplay between lattice and electronic properties. Co-author of more than 95 papers (H-Index: 21) and one book chapter.



**Dr. Joachim R. Binder** received the diploma degree in chemistry and the Ph.D. degree from the University of Osnabrück, Germany. In 1997, he joined the Forschungszentrum Karlsruhe (now Karlsruhe Institute of Technology), Germany, where he has been group leader at the Institute of Applied Materials since 1999. His current research is dedicated to synthesis and ceramic powder technology, especially for tunable microwave dielectrics, printed electronics and cathode materials for lithium and sodium ion batteries.



**Prof. Dr. Helmut Ehrenberg** is Professor for Inorganic Chemistry at the Karlsruhe Institute of Technology (KIT) and the Head of the Institute for Applied Materials (IAM). He addresses fundamentals and new materials for novel energy storage systems, development and processing of components for electrochemical energy storage devices and the integration of batteries into applications. He is a spokesperson of the cluster of excellence “Energy Storage beyond Lithium” (POLiS), a director of the Center for Electrochemical Energy Storage (CEL-EST) and speaker of the topic “Electrochemical Energy Storage” within the Helmholtz Association of German Research Centers (HGF).



**Dr. Sylvio Indris** is a group leader in the Institute for Applied Materials – Energy Storage Systems (IAM-ESS) at Karlsruhe Institute of Technology (KIT). He received his PhD in Physical Chemistry and Electrochemistry from Hannover University in 2001. Then he worked as post-doc at State University of New York at Stony Brook (SUNYSB) and subsequently he was head of a young-investigator group in the Institute of Nanotechnology (INT) of KIT. Sylvio Indris is working on electrode and electrolyte materials for Li-ion batteries with a focus on the elucidation of the fundamental electrochemical reaction mechanisms.